# Alkenone producers during late Oligocene-early Miocene revisited

Julien Plancq, Vincent Grossi, Jorijntje Henderiks, Laurent Simon, Emanuela Mattioli

# Alkenone producers during late Oligocene–early Miocene revisited

Julien Plancq,[1] Vincent Grossi,[1] Jorijntje Henderiks,[2] Laurent Simon,[3] and Emanuela Mattioli[1]

Received 10 May 2011; revised 8 September 2011; accepted 16 November 2011; published 18 January 2012.

[1] This study investigates ancient alkenone producers among the late Oligocene–early Miocene coccolithophores recorded at Deep Sea Drilling Project (DSDP) Site 516. Contrary to common assumptions, *Reticulofenestra* was not the most important alkenone producer throughout the studied time interval. The comparison between coccolith species-specific absolute abundances and alkenone contents in the same sedimentary samples shows that *Cyclicargolithus* abundances explain 40% of the total variance of alkenone concentration and that the species *Cyclicargolithus floridanus* was a major alkenone producer, although other related taxa may have also contributed to the alkenone production at DSDP Site 516. The distribution of the different alkenone isomers ($MeC_{37:2}$, $EtC_{38:2}$, and $MeC_{38:2}$) remained unchanged across distinct changes in species composition, suggesting similar diunsaturated alkenone compositions within the Noelaerhabdaceae family during the late Oligocene–early Miocene. However, the overall larger cell size of *Cyclicargolithus* may have implications for the alkenone-based reconstruction of past partial pressure of $CO_2$. Our results underscore the importance of a careful evaluation of the most likely alkenone producers for periods (>1.85 Ma) predating the first occurrence of contemporary alkenone producers (i.e., *Emiliania huxleyi* and *Gephyrocapsa oceanica*).

**Citation:** Plancq, J., V. Grossi, J. Henderiks, L. Simon, and E. Mattioli (2012), Alkenone producers during late Oligocene–early Miocene revisited, *Paleoceanography*, *27*, PA1202, doi:10.1029/2011PA002164.

## 1. Introduction

[2] Alkenones are long-chain ($C_{35}$–$C_{40}$) lipids whose biosynthesis in modern oceans is restricted to a few extant unicellular haptophyte algae belonging to the Isochrysidales clade, which includes the calcifying haptophytes (coccolithophores) *Emiliania huxleyi* and *Gephyrocapsa oceanica* [*Marlowe et al.*, 1984; *Volkman et al.*, 1980, 1995]. A few noncalcifying Isochrysidales, such as *Isochrysis galbana*, also produce alkenones but they are restricted to coastal areas and are not considered as an important source of alkenone in the open ocean [*Marlowe et al.*, 1990].

[3] Diunsaturated and triunsaturated $C_{37}$ alkenones ($C_{37:2}$ and $C_{37:3}$, respectively) are ubiquitous and abundant in marine sediments, and have been intensively used for paleoceanographic reconstructions [e.g., *Brassell et al.*, 1986; *Jasper and Hayes*, 1990; *Eglinton et al.*, 1992; *Bard et al.*, 1997; *Cacho et al.*, 1999; *Martrat et al.*, 2004; *Bolton et al.*, 2010]. The production of $C_{37:2}$ and $C_{37:3}$ alkenones is linked to the coccolithophore growth temperature [*Brassell et al.*, 1986; *Prahl and Wakeham*, 1987] and the so-called alkenone unsaturation index $U^{K'}_{37}$ (defined as the ratio $[C_{37:2}]/([C_{37:2}] + [C_{37:3}])$ has been used as a proxy to reconstruct past sea surface temperatures, especially during the Quaternary period [e.g., *Müller et al.*, 1998; *Eltgroth et al.*, 2005; *Pahnke and Sachs*, 2006]. The carbon isotopic composition of the $C_{37:2}$ alkenone ($\delta^{13}C_{37:2}$) is also used to evaluate the carbon isotopic fractionation ($\varepsilon_{p37:2}$) that occurred during marine haptophyte photosynthesis in order to estimate concentration of $CO_2$ in past ocean surface waters ($[CO_{2(aq)}]$) and partial pressure of atmospheric $CO_2$ (paleo-$pCO_2$) [e.g., *Jasper and Hayes*, 1990; *Jasper et al.*, 1994; *Bidigare et al.*, 1997, 1999; *Pagani et al.*, 1999; *Pagani*, 2002; *Seki et al.*, 2010].

[4] The alkenone-based proxies have been calibrated on modern coccolithophores in culture (*E. huxleyi* and *G. oceanica*) and on Quaternary sediments [e.g., *Conte et al.*, 1995, 1998; *Müller et al.*, 1998; *Popp et al.*, 1998; *Riebesell et al.*, 2000]. However, the temperature calibration of the $U^{K'}_{37}$ index is species-dependent [e.g., *Volkman et al.*, 1995; *Conte et al.*, 1998] and includes variability due to physiological factors such as nutrients and light availability [e.g., *Epstein et al.*, 1998; *Prahl et al.*, 2003]. Nutrient-limited chemostat cultures show that the carbon isotopic composition of alkenones and $\varepsilon_{p37:2}$ values vary with $[CO_{2(aq)}]$ and physiological factors such as growth rate ($\mu$) and cell size [*Laws et al.*, 1995; *Popp et al.*, 1998]. However, nutrient-

[1]Laboratoire de Géologie de Lyon, UMR 5276, CNRS, Université Lyon 1, Ecole Normale Supérieure Lyon, Villeurbanne, France.
[2]Paleobiology Program, Department of Earth Sciences, Uppsala University, Uppsala, Sweden.
[3]Laboratoire d'Ecologie des Hydrosystèmes Naturels et Anthropisés, UMR 5023, CNRS, Université Claude Bernard Lyon, Villeurbanne, France.


0883-8305/12/2011PA002164

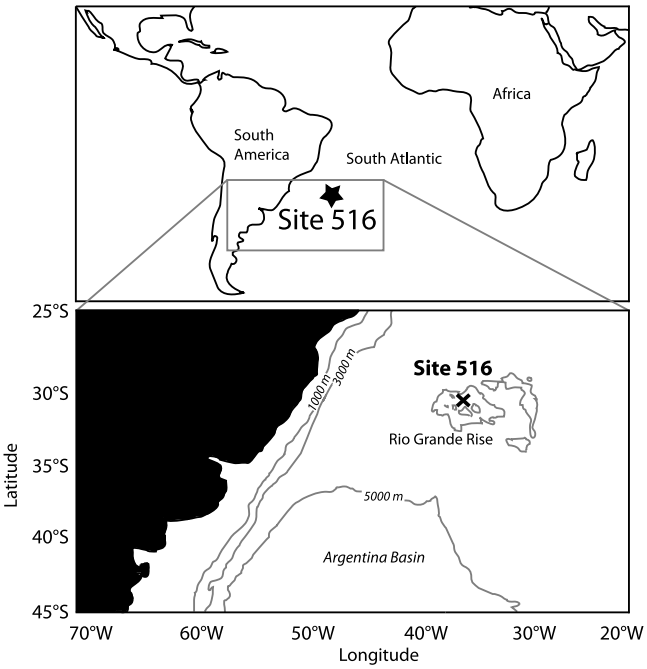


**Figure 1.** Location of DSDP Site 516 at the Rio Grande Rise (adapted from *Henderiks and Pagani* [2007]).

replete batch cultures produce much lower $\varepsilon_{p37:2}$ values and a different relationship between $\varepsilon_{p37:2}$ and $\mu/[CO_{2(aq)}]$ [*Riebesell et al.*, 2000].

[5] There is a huge gap between the first sedimentary record of alkenones in the Cretaceous at ~120 Ma [*Farrimond et al.*, 1986; *Brassell et al.*, 2004] and the first occurrence of modern alkenone producers (0.27 Ma for *E. huxleyi* [*Thierstein et al.*, 1977] and 1.85 Ma for *G. oceanica* [*Pujos-Lamy*, 1977]). Since *E. huxleyi* and *G. oceanica* cannot be responsible for alkenone production during most of the Cenozoic and the Mesozoic, the biological sources of alkenones preserved in pre-Quaternary sediments need to be elucidated in order to better constrain paleoenvironmental reconstructions based on these biomarkers.

[6] Based on the consistent cooccurrence of *Reticulofenestra* coccoliths and alkenones in marine sediments dating back to the Eocene (45 Ma), *Marlowe et al.* [1990] suggested that the most probable Cenozoic alkenone producers are to be found within the genus *Reticulofenestra*, which belongs to the Noelaerhabdaceae family like *Emiliania* and *Gephyrocapsa*. However, this study did not compare alkenone concentrations with *Reticulofenestra* absolute abundances. More recently, *Bolton et al.* [2010] argued that *Reticulofenestra* species were the main alkenone producers during the late Pliocene, based on a correlation between *Reticulofenestra* abundances and $C_{37}$ alkenone concentrations in sediments. Yet, other alkenones (e.g., $C_{38}$) were not considered.

[7] Here, we investigate the cooccurrence of alkenones and coccolithophore genera and species during the late Oligocene–early Miocene by comparing nannofossil assemblages and species-specific absolute abundances with alkenone contents ($C_{37}$ and $C_{38}$ alkenones) in sediments from the Deep Sea Drilling Project (DSDP) Site 516. This allows a detailed characterization of ancient alkenone producers and a reappraisal of paleoceanographic and paleo-$pCO_2$ reconstructions for the investigated period.

## 2. Material and Methods

### 2.1. Sampling

[8] DSDP Leg 72 Site 516 is located on the upper flanks of the Rio Grande Rise at 1313 m water depth in the South Atlantic subtropical gyre (Figure 1). Site 516 is situated north of the Northern Subtropical Front [*Belkin and Gordon*, 1996] and other front zones of the South Atlantic. During the Miocene, carbonate-rich sediments were deposited well above the lysocline and the calcite compensation depth (CCD), at water depths similar to today [*Barker*, 1983]. Studies by *Pagani et al.* [2000a, 2000b] and *Henderiks and Pagani* [2007] demonstrated the simultaneous presence of Noelaerhabdaceae coccoliths and alkenones in DSDP Site 516 sediment samples. However, these studies neither reported alkenone concentrations nor absolute abundances of coccoliths. We therefore selected a total of 35 sediment samples from Holes 516 and 516F. The sample depths slightly differ from those studied by *Henderiks and Pagani* [2007]. The time interval investigated spans the latest Oligocene and the early Miocene (25–16 Ma) and includes a period (~21–19 Ma) of major paleoceanographic changes [*Pagani et al.*, 2000b]. The age model for DSDP Site 516 used in this study is the one presented by *Henderiks and Pagani* [2007].

### 2.2. Total Organic Carbon Analyses

[9] Subsamples (~100 mg of ground bulk sediment) were acidified in situ with HCl 2N in precleaned (combustion at 450°C) silver capsules until effervescence ceased, dried in an oven (50°C) and wrapped in tin foil before analyses. Total organic carbon (TOC) analyses were performed with a Thermo FlashEA 1112 elemental analyzer using aspartic acid (36.09% of carbon) and nicotinamid (59.01% of carbon) as calibration standards (n = 5 with variable weight for each standard). Accuracy was checked using in-house reference material analyzed with the samples (fine ground low carbon sediment; 0.861 ± 0.034% of carbon (standard deviation; n = 12)). All samples were analyzed twice and the reproducibility achieved for duplicate analyses was better than 10% (coefficient of variation).

### 2.3. Alkenone Analyses

[10] Samples (~10 g) were ground and extracted by way of sonication (5×) using 50 mL of Dichloromethane (DCM)/Methanol (MeOH) (2:1 v/v). Following evaporation of the solvents, the total lipid extract was separated into three fractions using chromatography over a column of inactivated (4% $H_2O$) silica, with hexane (Hex), Hex/ethyl acetate (7:3 v/v) and DCM/MeOH (1:1 v/v) as eluents. The second fraction, containing alkenones, was dried under $N_2$, silylated (pyridine/N,O-bis(trimethylsilyl)trifluoroacetamide or BSTFA, 2:1 v/v, 60°C for 1 h) and dissolved in hexane for analysis by gas chromatography (GC/FID) and gas chromatography/mass spectrometry (GC/MS).

[11] Alkenones were identified by GC/MS using a MD800 Voyager spectrometer interfaced to an HP6890 gas

chromatograph equipped with an on-column injector and a DB-5MS column (30 m × 0.25 mm × 0.25 $\mu$m). The oven temperature was programmed from 60°C (1 min) to 130°C at 20°C $min^{-1}$, and then to 310°C (20 min) at 4°C $min^{-1}$. Helium was used as the carrier gas at constant flow (1.1 mL $min^{-1}$).

[12] Alkenone abundances were determined by GC/FID using hexatriacontane ($n$-$C_{36}$ alkane) as internal standard. The GC was a HP-6890 Series gas chromatograph configured with an on-column injector and a HP5 (30 m × 0.32 mm × 0.25 $\mu$m) capillary column. Helium was used as the carrier gas at constant flow and the oven temperature program was the same as for GC-MS analyses. Samples were injected twice and the reproducibility achieved for duplicate alkenone quantifications was less than 10% (coefficient of variation).

### 2.4. Micropaleontological Analyses

[13] Slides for calcareous nannofossil quantitative analysis were prepared following the random settling method [*Beaufort*, 1991b] (modified by *Geisen et al.* [1999]). A small amount of dried sediment powder (5 mg) was mixed with water (with basic pH, oversaturated with respect to calcium carbonate) and the homogenized suspension was allowed to settle for 24 h onto a cover slide. The slide was dried and mounted on a microscope slide with Rhodopass. Coccolith quantification was performed using a polarizing optical ZEISS microscope (magnification 1000×). A standard number of 500 calcareous nannofossils (coccoliths and nannoliths) were counted in a variable number (between 10 and 30) of field of views. In order to test the reproducibility of our quantification, each slide was counted twice and the reproducibility achieved was high (coefficient of variation: 10%).

[14] Absolute abundance of nannofossils per gram of sediment was calculated using the formula

$$X = (N*V)/(M*A*H), \quad (1)$$

where X is the number of calcareous nannofossils per gram of sediment; N the number of nannofossils counted in each sample; V the volume of water used for the dilution in the settling device (mL); M the weight of powder used for the suspension (g); A the surface considered for nannofossil counting ($cm^2$); H the height of the water over the cover slide in the settling device (2.1 cm). Species-specific relative abundances (percentages) were also calculated from the total nannofossil content.

[15] Coccolith size is a proxy for cell size in ancient Noelaerhabdaceae [*Henderiks*, 2008]. *Henderiks and Pagani* [2007] have already evaluated the size variability within the reticulofenestrids (namely species of the genera *Reticulofenestra* and *Dictyococcites*) at Site 516 and its implications for the interpretation of measured alkenone-based $\varepsilon_{p37:2}$ values. Here, we pair the reticulofenestrid size data with the mean size variability of *Cyclicargolithus* in the same 24 samples studied by *Henderiks and Pagani* [2007]. In each sample, 100 individual *Cyclicargolithus* coccoliths were measured from four replicate slides, rendering statistically robust estimates of mean size and its variance [*Henderiks and Törner*, 2006].

### 2.5. Comparison Between Alkenone and Nannofossil Contents

[16] Our working hypothesis is that, under good preservation conditions, the alkenone concentration should be related to the number of coccoliths of alkenone-producing taxa in sediments. A similar assumption has already been used to identify biological sources of alkenones in sediments of late Quaternary [e.g., *Müller et al.*, 1997; *Weaver et al.*, 1999] and Pliocene age [e.g., *Bolton et al.*, 2010; *Beltran et al.*, 2011]. Here, we compare major trends of absolute and relative abundances of coccolith genera to variations in total alkenone concentrations.

[17] Simple and multiple linear regression analyses (significance threshold $\alpha = 0.05$) were used to determine the relationships between alkenone contents and relative/absolute abundances of coccolith genera, and between $\varepsilon_{p37:2}$ (data from *Pagani et al.* [2000b]), abundances of coccolith genera and mean sizes. The normality of the input data and residual distributions was checked using a Shapiro-Wilk test. All statistical analyses were performed using the JMP version 8.0.1 (SAS institute) software.

## 3. Taxonomy Used for the Noelaerhabdaceae Family

[18] Since the early publication of *Marlowe et al.* [1990], the genus *Reticulofenestra* has been considered by different authors as the most probable alkenone producer during the Cenozoic. However, species of the genus *Reticulofenestra* are generally considered to have a high morphological plasticity, and the *Dictyococcites* and *Cyclicargolithus* genera are often considered as junior synonyms of *Reticulofenestra* [e.g., *Theodoridis*, 1984; *Marlowe et al.*, 1990; *Young*, 1990; *Aubry*, 1992; *Beaufort*, 1992; *Henderiks and Pagani*, 2007; *Henderiks*, 2008]. Consequently, these genera have often been grouped either as reticulofenestrids (*Reticulofenestra* + *Dictyococcites* [e.g., *Henderiks and Pagani*, 2007; *Henderiks*, 2008]) or more simply as *Reticulofenestra* (*Reticulofenestra* + *Dictyococcites* + *Cyclicargolithus* [e.g., *Aubry*, 1992]). This grouping can result in misleading conclusions when trying to precisely define ancient species involved in alkenone production. A taxonomic revision is beyond the scope of this work and *Dictyococcites*, *Reticulofenestra* and *Cyclicargolithus* are distinguished here on the basis of distinctive morphological features in optical microscope (Table 1 and Appendix A).

## 4. Results

### 4.1. TOC

[19] The studied samples are characterized by a low total organic carbon content (0.06% on average; Figure 2a). Higher values are recorded at the base of the studied interval and a slight trend to decreasing values is observed from 25 to 20 Ma, with a mean TOC content of 0.08% and 0.04% before and after 20.5 Ma, respectively (Figure 2a).

### 4.2. Alkenones

[20] One $C_{37}$ and two $C_{38}$ alkenones are present in all the samples studied. These were identified as heptatriacontadien-2-one ($MeC_{37:2}$), octatriacontadien-3-one ($EtC_{38:2}$) and octatriacontadien-2-one ($MeC_{38:2}$), respectively. $MeC_{37:2}$,

**Table 1.** Distinctive Morphological Features Used to Distinguish the Three Noelaerhabdaceae Genera (*Reticulofenestra, Dictyococcites,* and *Cyclicargolithus*) at DSDSP Site 516 During the Late Oligocene–Early Miocene

| Noelaerhabdaceae Genus | Distinctive Morphological Features |
|---|---|
| *Reticulofenestra* | Elliptical coccoliths with a prominent open central area and with no slits in the distal shield [*Hay et al.*, 1966]. |
| *Dictyococcites* | Elliptical coccoliths with a large central area closed or virtually closed in line with the distal shield. The central area of the distal shield frequently shows a median furrow or a minute pore [*Backman*, 1980]. |
| *Cyclicargolithus* | Circular to subcircular coccoliths with a small central area and high tube cycles [*Bukry*, 1971]. Larger coccolith size range than *Reticulofenestra* and *Dictyococcites* [*Henderiks*, 2008]. |

$EtC_{38:2}$, and $MeC_{38:2}$ alkenones account for 55%, 33%, and 12% of total alkenone content, respectively, and no significant variation of these proportions is observed through the time interval studied.

[21] The total amount of these ketones is relatively low (0.03 $\mu$g per gram of sediment on average), with a maximum of 0.13 $\mu$g per gram of sediment at about 23 Ma (Figure 2b), and values attaining the detection limit at around 20 and 17 Ma. A general trend to decreasing alkenone content is seen from 25 to 16 Ma but three periods of increasing total alkenone content are observed at about 23, 22–21.5 and 19.5–17.5 Ma (Figure 2b). This overall distribution matches with that of TOC (Figures 2a and 2b). The same variations are observed when each alkenone is considered individually. Similar trends also occur when alkenone content is expressed relative to TOC (Figure 2c). In Figure 3, quantitative alkenone data expressed per gram of sediment are compared to absolute and relative abundances of Noelaerhabdaceae coccoliths.

### 4.3. Coccolith Assemblages

[22] Coccoliths are well preserved in all investigated samples since delicate coccoliths that are prone to dissolution, such as *Syracosphaera* and *Pontosphaera*, are commonly observed with pristine structures. This indicates that coccolith assemblages are not importantly biased by selective dissolution in the water column or diagenetic effects, in agreement with previous studies at Site 516 [*Henderiks and Pagani*, 2007].

[23] The mean absolute abundance of nannofossils is $5.0 \times 10^9$ nannofossils per gram of sediment and does not show any significant stratigraphic trend across the late Oligocene–early Miocene (Figure 2d). Coccolith assemblages are dominated by four genera, which account for 70%–80% of the total assemblage, namely: *Reticulofenestra*, *Dictyococcites*, *Cyclicargolithus*, all belonging to the Noelaerhabdaceae family, and *Coccolithus*. No significant stratigraphic trend across the late Oligocene–early Miocene is observed when all the Noelaerhabdaceae are combined (Figure 2e). The mean absolute abundance of Noelaerhabdaceae is $3.4 \times 10^9$ coccoliths per gram of sediment (Figure 2e).

[24] For each genus of Noelaerhabdaceae, relative and absolute abundances show similar variations through time (Figures 3b, 3c, and 3d). Three shifts in coccolith assemblages can be distinguished: (1) Between 25 and 20.5 Ma, coccolith assemblages are dominated by *Cyclicargolithus* representing on average 30% ($1.4 \times 10^9$ specimens per gram of sediment) of the total nannofossil assemblage, whereas *Dictyococcites* represents ~25% ($1.3 \times 10^9$) and *Reticulofenestra* ~15% ($0.7 \times 10^9$); (2) between 20.5 and 17.5 Ma, coccolith assemblages show a dominance of *Dictyococcites* (40%; $2.3 \times 10^9$) and an increase (from 15% to 45%; $0.95 \times 10^9$ to $2.0 \times 10^9$) in the proportion of *Reticulofenestra*, whereas *Cyclicargolithus* shows a sharp decrease in abundance (8%; $0.42 \times 10^9$); and (3) assemblages between 17.5 and 16 Ma are characterized by the dominance of

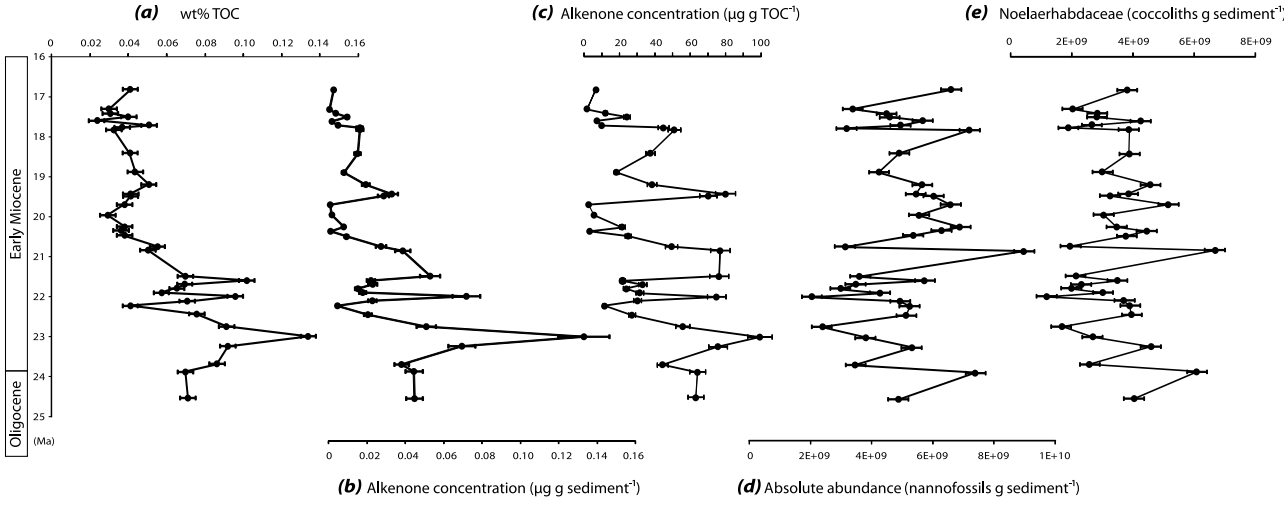


**Figure 2.** (a) Total organic carbon content (wt % TOC), (b) total alkenone content ($\mu$g per gram of sediment), (c) total alkenone content relative to TOC ($\mu$g per gram of TOC), (d) absolute abundance of nannofossils (specimens per gram of sediment), and (e) absolute abundance of Noelaerhabdaceae (coccoliths per gram of sediment) at DSDP Site 516 during the late Oligocene–early Miocene. Error bars represent coefficients of variation.

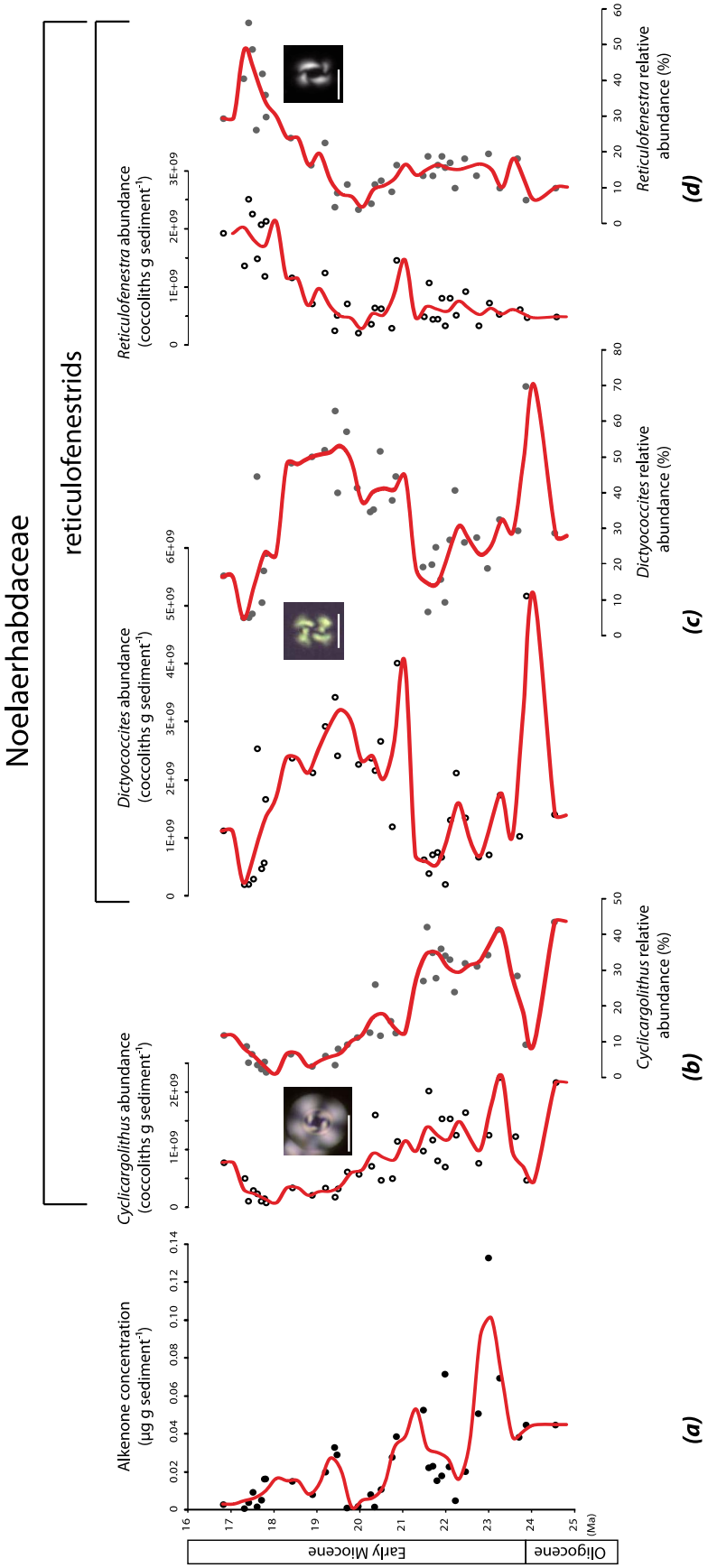


**Figure 3.** Comparison between alkenone concentration and Noelaerhabdaceae distribution at DSDP Site 516 during the late Oligocene–early Miocene. (a) Total alkenone content ($\mu$g per gram of sediment) and absolute and relative abundances of (b) *Cyclicargolithus*, (c) *Dictyococcites*, and (d) *Reticulofenestra*. Relative abundances are relative to the total nannofossil contents. Trend curves are moving average curves calculated using a 0.5 Ma window size and a 0.25 Ma time step. Scale bars on nannofossil pictures equal 4 $\mu$m.

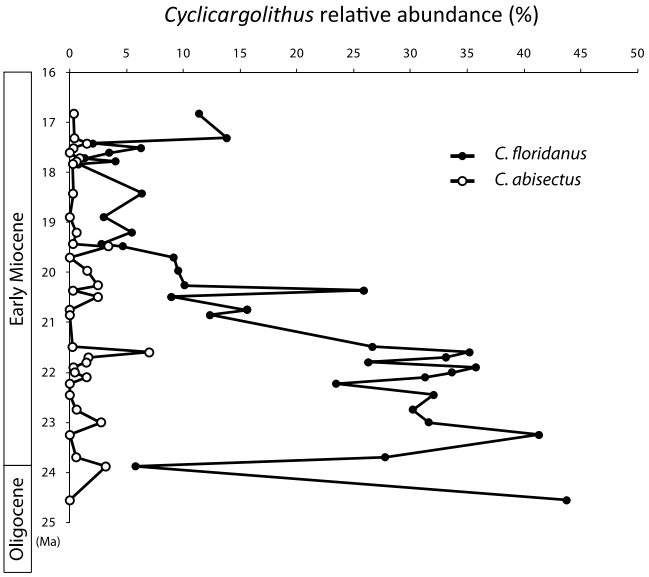


**Figure 4.** Relative abundances of *Cyclicargolithus* species *C. floridanus* and *C. abisectus* at DSDP Site 516. It should be noted that *C. floridanus* is entirely responsible for the *Cyclicargolithus* abundance trend.

*Reticulofenestra* (45%; $2.0 \times 10^9$) with smaller amounts of both *Cyclicargolithus* (9%; $0.44 \times 10^9$) and *Dictyococcites* (8%; $0.42 \times 10^9$). In general, *Dictyococcites* and *Cyclicargolithus* abundances show opposite trends (Figures 3b and 3c). This record is consistent with the results of *Henderiks and Pagani* [2007] although the apparent timing in assemblage shifts is slightly different due to different sample spacing.

[25] The coccolith size of *Cyclicargolithus*, which is strongly linearly correlated to its cell diameter [*Henderiks*, 2008], ranges between 4 and 12 $\mu$m (N = 2454). Mean size per sample varies between 6.13 $\mu$m $\pm$ 0.24 (95% confidence mean) in the late Oligocene and 8.45 $\mu$m $\pm$ 0.18 (95% confidence mean) in the early Miocene.

## 5. Discussion

### 5.1. Alkenone Producers at DSDP Site 516

[26] Significant correlations between the abundance of coccoliths of the main alkone producers (namely *E. huxleyi* and *G. oceanica*) and the alkenone concentration have been observed in late Quaternary sediments [e.g., *Müller et al.*, 1997; *Weaver et al.*, 1999]. Based on this observation, parallel distributions of reticulofenestrid coccoliths and alkenone contents have been used to identify past biological sources of alkenones in Pliocene sediments [e.g., *Bolton et al.*, 2010; *Beltran et al.*, 2011]. The similar variations at DSDP Site 516 between the absolute abundance of *Cyclicargolithus* coccoliths and the total alkenone content (Figure 3) suggests a significant contribution of this genus to alkenone production between 25 and 16 Ma. More precisely, alkenone production is supported by the species *C. floridanus* which is entirely responsible for the *Cyclicargolithus* abundance trend (Figure 4). Although reticulofenestrids are sometimes considered as species having high morphological plasticity which may bias their taxonomy [e.g., *Beaufort*, 1991a], *C. floridanus* represents a very characteristic morphospecies easily distinguishable from other reticulofenestrids due to its larger size and distinct subcircular shape.

[27] Processes of degradation in the water column and in sediments may affect alkenone and coccolith records differently, leading to misleading interpretations of the sedimentary record. In the present case, several observations argue against the effects of such potential preservation biases.

[28] First, records of coccolith assemblages can be skewed by the dissolution of susceptible species during settling and sedimentary burial [*Roth and Coulbourn*, 1982; *Gibbs et al.*, 2004; *Young et al.*, 2005]. Such selective coccolith dissolution is not observed within the studied nannofossil groups at DSDP Site 516 [*Henderiks and Pagani*, 2007; this study]. Sediments from Site 516 are calcareous oozes with little evidence of dissolution or cementation precipitation [*Barker et al.*, 1983], and no significant secondary calcite overgrowth is observed on coccoliths [*Ennyu et al.*, 2002]. An important effect of diagenesis affecting the recorded coccolith assemblages can thus be excluded.

[29] Second, a majority of organic matter produced in the surface oceans is generally remineralized before and after reaching the seafloor. The concentrations of TOC and alkenones in sediments are thus a function of preservation conditions and represent only a fraction of the original export productivity. Nevertheless, the relatively high sedimentation rate (17 m/Ma) and the relatively shallow water depth (1313 m) of DSDP Site 516 [*Barker et al.*, 1983] induced a limited oxidation and a relatively rapid burial of organic matter into the sediments compared to other oceanic settings [*Mukhopadhyay et al.*, 1983]. Moreover, the paleodepth of the studied site did not change significantly during the time span investigated. Changes in TOC and alkenone concentrations in sediments may also reflect varying sedimentation rate. However, the sedimentation rate calculated according to the age model of the studied interval does not show significant variations [*Pagani et al.*, 2000b; *Henderiks and Pagani*, 2007]. Thus the observed overall decrease in TOC since ~21.5 Ma (Figure 2a) likely reflects a decrease in primary productivity in response to paleoceanographic changes (mainly linked to temperature and nutrient concentrations [*Pagani et al.*, 2000b; *Henderiks and Pagani*, 2007]) rather than changes in sedimentary dilution or organic matter degradation. Despite the fact that alkenones represent only a very small fraction of TOC, the significant covariation observed between TOC and total alkenone content (Figures 2a and 2b; $R^2 = 0.69$, $p < 0.0001$) suggests that alkenone distribution also reflects variations in the abundance of alkenone producers rather than an erratic degradation of alkenones relative to TOC. It should be noted that these biolipids are generally considered less prone to degradation than other phytoplankton-derived lipids [*Sun and Wakeham*, 1994; *Gong and Hollander*, 1997, 1999]. In addition, the association between organic matter and the calcium carbonate of coccoliths might have produced a physical and chemical protection against remineralization [*Armstrong et al.*, 2002], as coccoliths have very likely acted as ballast and reduced the residence time of organic matter within the water column [*Klaas and Archer*, 2002].

[30] Finally, the apparent similar variations between the abundance of *Cyclicargolithus* and the total alkenone content are supported by statistical analyses which show that, among all tested Noelaerhabdaceae genera, only absolute

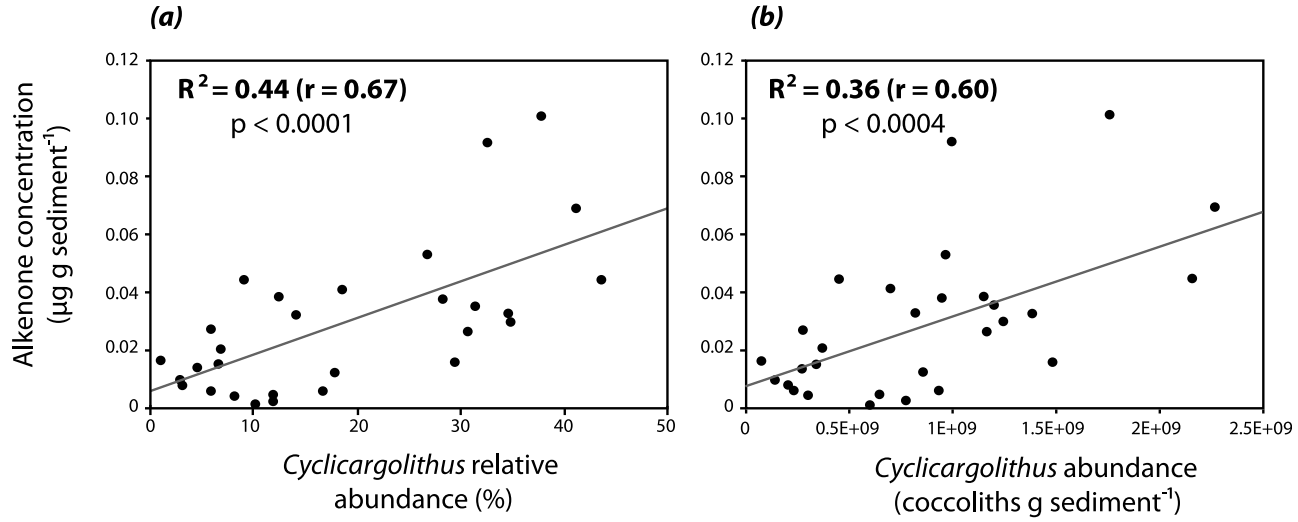


**Figure 5.** Correlations (linear regressions; $\alpha = 0.05$) between alkenone content ($\mu$g per gram of sediment) and (a) relative and (b) absolute abundances of *Cyclicargolithus* during the late Oligocene–early Miocene at DSDP Site 516.

and relative abundances of this genus produce significant and positive linear correlations with the total alkenone content ($R^2$ = 0.36–0.44, $p < 0.0005$; Figure 5). Such a correlation is unlikely the result of diagenetic processes. Still, it is possible that a better preservation of the calcite of coccoliths compared to alkenones has led to an underestimation of the contribution of *Cyclicargolithus* to alkenone production. This may partly explain why *Cyclicargolithus* represents only 40% of the total variance of alkenone concentration. However, other taxa may have also contributed to the alkenone production at DSDP Site 516 since *Cyclicargolithus* has a limited stratigraphical range (from ~40 Ma to ~13 Ma [*Young*, 1998]). The continuous cooccurrence of the *Reticulofenestra* genus and alkenones throughout the Cenozoic sediment record is the main argument to infer it is the most probable ancient alkenone producer [e.g., *Marlowe et al.*, 1990]. In the present study, the quantitative distribution of *Reticulofenestra* shows an inverse trend compared to that of alkenone concentrations (Figures 3a and 3d). Moreover, when considering *Reticulofenestra* plus *Cyclicargolithus* abundances in a multiple linear regression calculated versus alkenone concentrations, the fit does not increase ($R^2 = 0.45$, $p < 0.001$) with respect to *Cyclicargolithus* alone ($R^2 = 0.44$, $p < 0.0005$). These observations suggest a weak contribution of the genus *Reticulofenestra* to alkenone production in the time interval considered, although a contribution of this genus cannot be completely excluded. Abundances of *Dictyoccocites* (Figure 3c) do not significantly correlate either with the general trend of alkenone concentrations. However, a contribution of *Dictyococcites* to alkenone production cannot be excluded especially after 20.5 Ma where a small increase in alkenone content coincides with a sharp increase in *Dictyococcites* (Figures 3a and 3c). It is also possible that noncalcifying haptophytes, for which there is no mineralized fossil record, have contributed to the alkenone production at DSDP Site 516 although extant noncalcifying alkenone producers (e.g., *Isochrysis galbana*) are not considered as an important source of alkenones in modern open ocean sediments [*Marlowe et al.*, 1990].

[31] It is worth noticing that no change in the proportion of the different alkenone isomers ($MeC_{37:2}$, $EtC_{38:2}$, and $MeC_{38:2}$) is observed throughout the entire time interval considered in this study. This may imply that all alkenone-producing species produced the same type of alkenones during the late Oligocene–Early Miocene, which may not be surprising since the alkenone compositions of modern coccolithophorids (essentially *G. oceanica* and *E. huxleyi*) are rather similar [*Volkman et al.*, 1995]. It is possible, however, that the original distribution of alkenones at DSDP Site 516 contained alkenone isomers with more than two unsaturations, since triunsaturated and tetraunsaturated alkenones are known to be far more reactive toward diagenetic processes than their diunsaturated homologues [e.g., *Grimalt et al.*, 2000; *Rontani and Wakeham*, 2008].

### 5.2. Paleoenvironmental Implications

[32] Past atmospheric $CO_2$ concentrations ($pCO_2$) can be estimated from the carbon isotopic fractionation between ambient $CO_2$ and the algal cell ($\varepsilon_{p37:2}$) that occurred during marine haptophyte photosynthesis [*Jasper and Hayes*, 1990; *Jasper et al.*, 1994; *Bidigare et al.*, 1997, 1999; *Pagani et al.*, 1999], based on the expression

$$\varepsilon_{p37:2} = \varepsilon_f - b/[CO_{2(aq)}], \quad (2)$$

where $\varepsilon_{p37:2}$ is calculated from the difference between the carbon isotopic compositions of diunsturated $C_{37}$ alkenone ($\delta^{13}C_{37:2}$) and foraminifera carbonate ($\delta^{13}C_{foram}$) [see *Pagani et al.*, 1999]. $\varepsilon_f$ is the carbon isotope fractionation due to all carbon-fixing reactions (here assuming $\varepsilon_f$ = 25‰ [*Popp et al.*, 1998]) and '*b*' represents the sum of physiological factors, including growth rate and cell geometry, that affect total carbon isotope discrimination [*Laws et al.*, 1995; *Popp et al.*, 1998]. The magnitude of term '*b*' is estimated by the phosphate concentration of the surface ocean [*Bidigare et al.*, 1997, 1999; *Pagani et al.*, 1999]. In oligotrophic settings, it is generally assumed that the influence of

**Table 2.** Pairwise Linear Regressions Between Alkenone $\delta^{13}C$ ($\delta^{13}C_{37:2}$), $\varepsilon_{p37:2}$, *Cyclicargolithus* and Reticulofenestrids Mean Cell Size, and the Ratio of *Cyclicargolithus* to Noelaerhabdaceae

| | $\delta^{13}C_{37:2}$ | $\varepsilon_{p37:2}$ | Reticulofenestrid Mean Size | *Cyclicargolithus* Mean Size | Mix Mean Size |
|---|---|---|---|---|---|
| $\varepsilon_{p37:2}$ | $R = -0.96$<br>$p < 0.0001$ | | | | |
| Reticulofenestrid mean size | $R = 0.68$<br>$p = 0.0003$ | $R = -0.68$<br>$p = 0.0003$ | | | |
| *Cyclicargolithus* mean size | $R = 0.69$<br>$p = 0.0002$ | $R = -0.67$<br>$p = 0.0004$ | $R = 0.75$<br>$p < 0.0001$ | | |
| Mix mean size | $R = 0.33$<br>$p = 0.112$ | $R = -0.36$<br>$p = 0.085$ | $R = 0.86$<br>$p < 0.0001$ | $R = 0.50$<br>$p = 0.013$ | |
| *Cyclicargolithus*/ Noelaerhabdaceae | $R = -0.67$<br>$p = 0.0003$ | $R = 0.62$<br>$p = 0.0013$ | $R = -0.34$<br>$p = 0.099$ | $R = -0.60$<br>$p = 0.002$ | $R = -0.17$<br>$p = 0.419$ |

haptophyte growth rates on $\varepsilon_{p37:2}$ is negligible [e.g., *Pagani et al.*, 2005].

[33] Considering that larger phytoplankton cells, with higher carbon cell quota relative to surface area, fractionate less than smaller cells under similar $CO_{2(aq)}$ and low growth rates [e.g., *Laws et al.*, 1995; *Popp et al.*, 1998], *Henderiks and Pagani* [2007] applied a cell size correction to the term '*b*' in order to revise $pCO_2$ trends reconstructed by *Pagani et al.* [2000b] at DSDP Site 516. This correction was based on the cell diameter of reticulofenestrids, namely *Reticulofenestra* and *Dictyococcites*, considered as the most probable alkenone producers during the Cenozoic. Indeed, a significant correlation exists between alkenone $\delta^{13}C_{37:2}$ (and therefore $\varepsilon_{p37:2}$) and reticulofenestrid mean size ($R = 0.68$, $p = 0.0003$; Table 2). Yet, the present study suggests that another major alkenone producer at

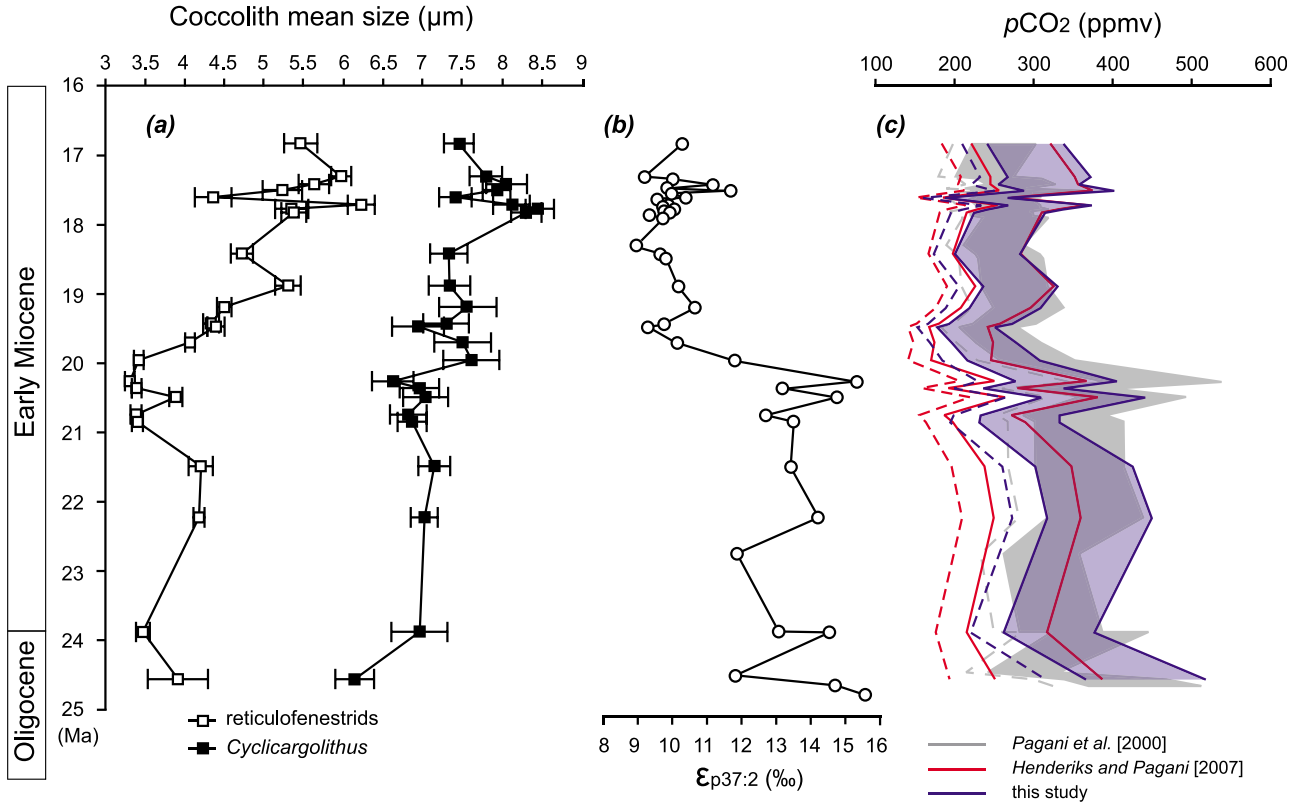


**Figure 6.** (a) Mean size variability at Site 516 of reticulofenestrids (*Reticulofenestra* plus *Dictyococcites*) and *Cyclicargolithus*, as determined in the 24 samples studied by *Henderiks and Pagani* [2007] (error bars indicate 95% confidence intervals); (b) alkenone-derived $\varepsilon_{p37:2}$ record [from *Pagani et al.*, 2000b]; (c) revised $pCO_2$ estimates after cell size corrections (see detailed methods in work by *Henderiks and Pagani* [2007]) including *Cyclicargolithus* (blue) compared to $pCO_2$ estimates of *Pagani et al.* [2000b] (grey) and *Henderiks and Pagani* [2007] (red). Shaded bands and lines depict minimum and maximum estimates with propagated 95% confidence levels of input factors. Dashed lines represent minimum estimates assuming no diagenetic alteration of biogenic carbonates used to determine paleo-SST [see *Pagani et al.*, 2005].

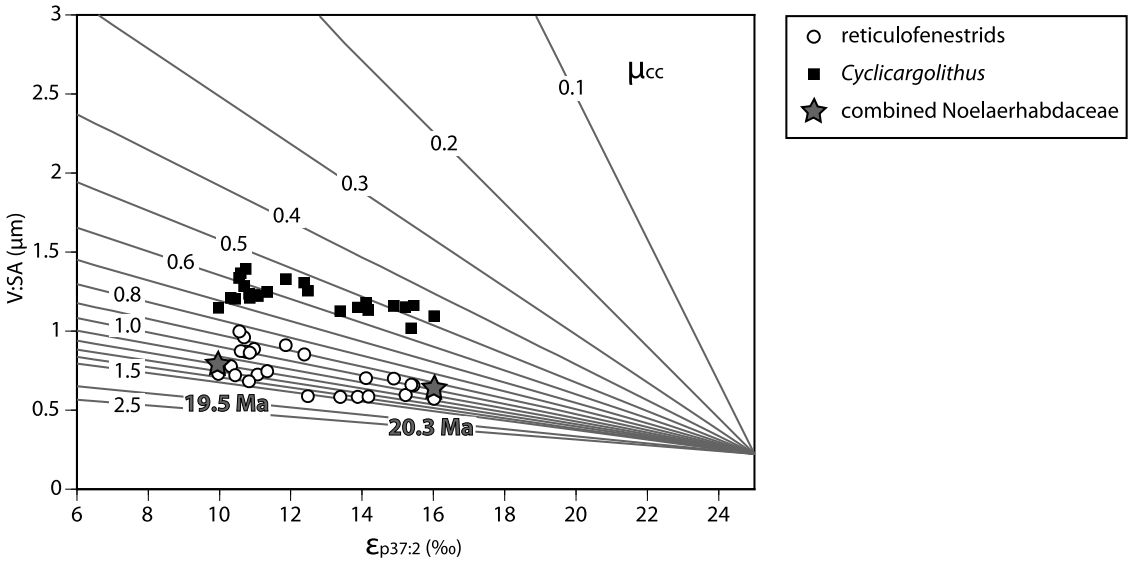


**Figure 7.** Relationship between $\varepsilon_{p37:2}$ (‰), cell volume to surface area ratios (V:SA; $\mu$m), and growth rates ($\mu_{cc}$; $d^{-1}$), calculated with constant $CO_{2(aq)}$ = 10 $\mu$mol $kg^{-1}$ [after *Henderiks and Pagani*, 2007]. The contoured growth rates represent values under continuous light chemostat experiments and need to be corrected for the effect of day length and respiration in natural settings [*Bidigare et al.*, 1997, 1999]. The stars depict the 6‰ decrease in $\varepsilon_{p37:2}$ between 20.3 and 19.5 Ma, which, under constant $CO_2$, corresponds to an increase in Noelaerhabdaceae cell sizes and growth rates.

this site was *Cyclicargolithus*, which had an overall larger cell diameter than the reticulofenestrids (Figure 6a). We have thus reevaluated the interpretation of published $\varepsilon_{p37:2}$ values (Figure 6b) [*Pagani et al.*, 2000b] and reestimated paleo-$pCO_2$ values considering the mean cell size of *Cyclicargolithus*. Prior to 20 Ma, this results in higher $pCO_2$ estimates (max. 340–550 ppmv) compared to values presented by *Henderiks and Pagani* [2007] due to the relatively high proportions and larger size of *Cyclicargolithus*. After 20 Ma, *Cyclicargolithus* is less common than large reticulofenestrids, resulting in $pCO_2$ estimates (<400 ppmv) that are similar to those determined by *Henderiks and Pagani* [2007]. Overall, the new $pCO_2$ estimates stay within the ranges previously reported by *Pagani et al.* [2000b] (Figure 6c).

[34] Relative differences in growth rates between reticulofenestrids and *Cyclicargolithus* can be evaluated using the following model [*Henderiks and Pagani*, 2007]:

$$\mu/[CO_{2(aq)}] = (\varepsilon_{p37:2} - \varepsilon_f)/K_{V:SA,} \quad (3)$$

where the term '*b*' from equation (2) is now expressed by specific growth rate ($\mu$) and a constant ($K_{V:SA}$) that is defined by the cell volume to surface area ratio (V:SA) of eukaryotic species [*Popp et al.*, 1998]

$$K_{V:SA} = 49 - 222(V:SA). \quad (4)$$

[35] Under constant [$CO_{2(aq)}$], and assuming no vital effects in $\varepsilon_{p37:2}$ between different haptophytes, similar values of $\varepsilon_{p37:2}$ could be generated by large cells (high V:SA) with low growth rates and/or small cells with high growth rates (Figure 7). In this scenario, our reconstructions indicate that *Cyclicargolithus* had 30% to 60% lower specific growth rates than the reticulofenestrids.

[36] Without access to cell geometry data and detailed nannofossil data, *Pagani et al.* [2000b] initially calculated an overall ~60% increase in haptophyte growth rates to explain the distinct 6‰ decrease in $\varepsilon_{p37:2}$ observed after ~20 Ma (Figure 6b). Here we combine the *Cyclicargolithus* and reticulofenestrid data (based on their mean size and respective proportions relative to the total Noelaerhabdaceae abundance), and show that the 6‰ shift in $\varepsilon_{p37:2}$ is supported by an increase (~23%) in mean cell size (V:SA) and by an overall increase in mean growth rates of ~24% (Figure 7). The distinct 6‰ shift in $\varepsilon_{p37:2}$ may thus be partly explained by changes in the major alkenone producers with different growth rates under similar $CO_2$ conditions: from assemblages dominated by slow-growing *Cyclicargolithus* to dominantly reticulofenestrids with higher growth rates. Pairwise correlations (Table 2) show that there is a significant correlation between $\delta^{13}C_{37:2}$ (and therefore $\varepsilon_{p37:2}$) and reticulofenestrid mean size ($R$ = 0.68, $p < 0.001$); $\delta^{13}C_{37:2}$ and *Cyclicargolithus* mean size ($R$ = 0.69, $p$ = 0.0002); and $\delta^{13}C_{37:2}$ and the *Cyclicargolithus*/Noelaerhabdaceae abundance ratio ($R$ = −0.67, $p$ = 0.0003). Finally, the observed variability in alkenone $\delta^{13}C_{37:2}$ and $\varepsilon_{p37:2}$ are best explained by a multiple linear regression linking the $\delta^{13}C_{37:2}$ to changes in mean Noelaerhabdaceae cell size and in the *Cyclicargolithus*/Noelaerhabdaceae abundance ratio ($R$ = 0.81; $p < 0.0001$).

## 6. Conclusion

[37] A comparison of nannofossil and alkenone absolute contents in Atlantic sediment samples (DSDP Site 516) spanning the late Oligocene to early Miocene suggests that the species *Cyclicargolithus floridanus* was a major alkenone

producer between 25 and 20.5 Ma, explaining at least 40% of the total alkenone content at this site. The contribution to alkenone production by large *Dictyococcites* is supported in younger sediments whereas that of *Reticulofenestra* species appears less pronounced. These observations challenge previous statements that *Reticulofenestra* was the most important alkenone producer during the late Oligocene–early Miocene. The relatively high proportions of *Cyclicargolithus* before 20 Ma and its larger cell size lead to higher paleo-$pCO_2$ estimates than those previously determined without considering this genus. Finally, the variability in alkenone $\delta^{13}C_{37:2}$ and $\varepsilon_{p37:2}$ are explained by changes in mean cell size as well as changes in the major alkenone producers with different growth rates. This highlights the importance of a careful evaluation of the most likely alkenone producers before using alkenone-based proxies for paleoenvironmental reconstructions.

## Appendix A: Taxonomic Remarks

[38] Taxonomy used in the present work follows Haptophyte phylogeny as revised by *Young and Bown* [1997] and *Sáez et al.* [2004].

### A1. Noelaerhabdaceae Family

[39] *Noelaerhabdaceae* (*Jerkovic* [1970], emended by *Young and Bown* [1997]) is the dominant family in most Neogene assemblages, considered as the Cenozoic ancestor of the modern alkenone producers *Emiliania* and *Gephyrocapsa*.

#### A1.1. Genus *Reticulofenestra*

[40] Elliptical to subcircular coccoliths with a prominent open central area and with no slits in the distal shield. The rather simple morphology of *Reticulofenestra* [*Hay et al.*, 1966] makes subdivision into species notoriously problematic. The conventional taxonomy is primarily based on size. This is unsatisfactorily and arbitrary, but of stratigraphic value [*Backman*, 1980; *Young et al.*, 2003]. In this study, a subdivision of four size-defined species was employed during the assemblage counts: (1) *Reticulofenestra haqii* [*Backman*, 1978]: morphospecies 3–5 $\mu$m in length, with a central opening shorter than 1.5 $\mu$m; (2) *Reticulofenestra minuta* [*Roth*, 1970]: morphospecies smaller than 3 $\mu$m; (3) *Reticulofenestra minutula* [*Gartner*, 1967; *Haq and Berggren*, 1978]: morphospecies 3–5 $\mu$m in length with a central opening longer than 1.5 $\mu$m; and (4) *Reticulofenestra pseudoumbilicus* [*Gartner*, 1967, 1969]: larger morphospecies (5–7 $\mu$m).

#### A1.2. Genus *Dictyococcites*

[41] Elliptical coccoliths with a large central area closed (or virtually closed) in line with the distal shield. The central area of the distal shield frequently shows a median furrow or a minute pore, but not large enough to suggest that they belong to *Reticulofenestra*. Although *Dictyococcites sensu* [*Black*, 1967] can be regarded as a heavily calcified, junior synonym of *Reticulofenestra*, the emended diagnosis of *Backman* [1980] clearly separates this genus from *Reticulofenestra*.

[42] *Dictyococcites* spp. are small morphospecies (<3 $\mu$m) with a supposed closed central area.

[43] *Dictyococcites antarcticus* [*Haq*, 1976]: in contrast with *D. hesslandii*, the specimens of *D. antarcticus* (4–8 $\mu$m) show no pore but a narrow and elongated rectangular central area (named "furrow" by *Haq* [1976] and "straight band" by *Backman* [1980]). The straight extinction band along the major axis occupies at least one half of the total length of the elliptical central area [*Backman*, 1980].

[44] *Dictyococcites hesslandii* [*Haq*, 1966; *Haq and Lohmann*, 1976]: for these specimens, the central area of the distal shield exhibits a small pore, from which extinction bands radiate (3–8 $\mu$m). Two morphometric size classes were distinguished in this study (3–5 $\mu$m and >5 $\mu$m).

#### A1.3. Genus *Cyclicargolithus*

[45] This genus is represented by circular to subcircular coccoliths with a small central area and high tube cycles. Although *Theodoridis* [1984] assigned *Cyclicargolithus* as a junior synonym of *Reticulofenestra*, the emended diagnosis of *Bukry* [1971] clearly separates this genus from *Reticulofenestra*.

[46] *Cyclicargolithus abisectus* [*Müller*, 1970; *Wise*, 1973] are large species (>10 $\mu$m).

[47] *Cyclicargolithus floridanus* [*Hay et al.*, 1967; *Bukry*, 1971] are species smaller than 10 $\mu$m.

### A2. Other Coccoliths

[48] Other coccoliths that do not belong to the Noelaerhabdaceae family and found in the studied samples are listed here: *Calcidiscus leptoporus* [*Murray and Blackman*, 1898; *Loeblich and Tappan*, 1978], *Coccolithus miopelagicus* [*Bukry*, 1971], *Coccolithus pelagicus* [*Wallich*, 1877; *Schiller*, 1930], *Helicosphaera* spp. [*Kamptner*, 1954], *Pontosphaera* spp. [*Lohmann*, 1902], *Syracosphaera pulchra* [*Lohmann*, 1902], and *Umbilicosphaera* spp. [*Lohmann*, 1902].

### A3. Nannoliths

[49] Nannoliths are thought to be related to coccoliths but have peculiar structures. Nannoliths found in the studied samples are *Discoaster* spp. [*Tan*, 1927] and *Sphenolithus* spp. [*Grassé*, 1952].

[50] **Acknowledgments.** We would like to thank two anonymous reviewers for their constructive comments and critical review. This study used Deep Sea Drilling Project samples provided by the Integrated Ocean Drilling Program. We thank Walter Hale from the Bremen Core Repository for his efficiency.

## References

Armstrong, R. A., C. Lee, J. I. Hedges, S. Honjo, and S. G. Wakeham (2002), A new mechanistic model for organic carbon fluxes in the ocean based on the quantitative association of POC with ballast minerals, *Deep Sea Res. Part II*, *49*, 219–236, doi:10.1016/S0967-0645(01)00101-1.

Aubry, M. P. (1992), Paleogene calcareous nannofossils from the Kerguelen Plateau, Leg 120, *Proc. Ocean Drill. Program Sci. Results*, *120*, 471–491, doi:10.2973/odp.proc.sr.120.149.1992.

Backman, J. (1978), Late Miocene–early Pliocene nannofossil biochronology and biogeography in the Vera Basin, SE Spain, *Stockholm Contrib. Geol.*, *32*, 93–114.

Backman, J. (1980), Miocene-Pliocene nannofossils and sedimentation rates in the Hatton-Rockall basin, NE Atlantic Ocean, *Stockholm Contrib. Geol.*, *36*(1), 1–91.

Bard, E., F. Rostek, and C. Sonzogni (1997), Interhemispheric synchrony of the last deglaciation inferred from alkenone paleothermometry, *Nature*, *385*, 707–710, doi:10.1038/385707a0.

Barker, P. F. (1983), Tectonic evolution and subsidence history of the Rio Grande Rise, *Initial Rep. Deep Sea Drill. Proj.*, *72*, 953–976, doi:10.2973/dsdp.proc.72.151.1983.

Barker, P. F. et al. (1983), Site 516: Rio Grande Rise, *Initial Rep. Deep Sea Drill. Proj.*, *72*, 155–338, doi:10.2973/dsdp.proc.72.105.1983.

Beaufort, L. (1991a), Dynamique du nannoplancton calcaire au cours du Néogène: Implication climatiques et océanographiques, MS thesis, 173 pp., Lab de Geol. de Lyon, Univ. Lyon, Lyon, France.

Beaufort, L. (1991b), Adaptation of the random settling method for quantitative studies of calcareous nannofossils, *Micropaleontology*, *37*, 415–418, doi:10.2307/1485914.

Beaufort, L. (1992), Size variations in late Miocene *Reticulofenestra* and implication for paleoclimatic interpretation, *Mem. Sci. Geol.*, *43*, 339–350.

Belkin, I. M., and A. L. Gordon (1996), Southern Ocean fronts from the Greenwich meridian to Tasmania, *J. Geophys. Res.*, *101*, 3675–3696, doi:10.1029/95JC02750.

Beltran, C., J.-A. Flores, M.-A. Sicre, F. Baudin, M. Renard, and M. de Rafélis (2011), Long chain alkenones in the early Pliocene Sicilian sediments (Trubi Formation–Punta di Maiata section): Implications for the alkenone paleothermometry, *Palaeogeogr. Palaeoclimatol. Palaeoecol.*, *308*, 253–263, doi:10.1016/j.palaeo.2011.03.017.

Bidigare, R. R., et al. (1997), Consistent fractionation of $^{13}C$ in nature and in the laboratory: Growth-rate effects in some haptophyte algae, *Global Biogeochem. Cycles*, *11*, 279–292, doi:10.1029/96GB03939.

Bidigare, R. R., et al. (1999), Correction to "Consistent fractionation of $^{13}C$ in nature and in the laboratory: Growth-rate effects in some haptophyte algae," *Global Biogeochem. Cycles*, *13*, 251– 252, doi:10.1029/1998GB900011.

Black, M. (1967), New names for some coccolith taxa, *Proc. Geol. Soc. Lond.*, *1640*, 139–145.

Bolton, C. T., K. T. Lawrence, S. J. Gibbs, P. A. Wilson, L. C. Cleaveland, D. Timothy, and T. D. Herbert (2010), Glacial-interglacial productivity changes recorded by alkenones and microfossils in late Pliocene eastern equatorial Pacific and Atlantic upwelling zones, *Earth Planet. Sci. Lett.*, *295*, 401–411, doi:10.1016/j.epsl.2010.04.014.

Brassell, S. C., G. Eglinton, I. T. Marlowe, U. Pflaumann, and M. Sarnthein (1986), Molecular stratigraphy: A new tool for climatic assessment, *Nature*, *320*, 129–133, doi:10.1038/320129a0.

Brassell, S. C., M. Dumitrescu, and the ODP Leg 198 Shipboard Scientific Party (2004), Recognition of alkenones in a lower Aptian porcellanite from the west-central Pacific, *Org. Geochem.*, *35*, 181–188, doi:10.1016/j.orggeochem.2003.09.003.

Bukry, D. (1971), Cenozoic calcareous nannofossils from the Pacific Ocean, *Trans. San Diego Soc. Nat. Hist.*, *16*, 303–327.

Cacho, I., J. O. Grimalt, C. Pelejero, M. Canals, F. J. Sierro, J. A. Flores, and N. J. Shackleton (1999), Dansgaard-Oeschger and Heinrich event imprints in Alboran Sea paleotemperatures, *Paleoceanography*, *14*, 698–705, doi:10.1029/1999PA900044.

Conte, M. H., A. Thompson, and G. Eglinton (1995), Lipid biomarker diversity in the coccolithophorid *Emiliania huxleyi* (Prymnesiophycea) and the related species *Gephyrocapsa oceanica*, *J. Phycol.*, *31*, 272–282, doi:10.1111/j.0022-3646.1995.00272.x.

Conte, M. H., A. Thompson, D. Lesley, and R. P. Harris (1998), Genetic and physiological influences on the alkenone/alkenoate versus growth temperature relationship in *Emiliania huxleyi* and *Gephyrocapsa oceanica*, *Geochim. Cosmochim. Acta*, *62*(1), 51–68, doi:10.1016/S0016-7037(97)00327-X.

Eglinton, G., S. A. Bradshaw, A. Rosell, M. Sarnthein, U. Pflaumann, and R. Tiedemann (1992), Molecular record of secular sea surface temperature changes on 100-year timescales for glacial terminations I, II and IV, *Nature*, *356*, 423–426, doi:10.1038/356423a0.

Eltgroth, M. L., R. L. Watwood, and G. V. Wolfe (2005), Production and cellular localisation of neutral long-chain lipids in the haptophyte algae *Isochrysis galbana* and *Emiliania huxleyi*, *J. Phycol.*, *41*, 1000–1009, doi:10.1111/j.1529-8817.2005.00128.x.

Ennyu, A., M. A. Arthur, and M. Pagani (2002), Fine-fraction carbonate stable isotopes as indicators of seasonal shallow mixed-layer paleohydrography, *Mar. Micropaleontol.*, *46*, 317–342, doi:10.1016/S0377-8398(02)00079-8.

Epstein, B. L., S. D'Hondt, J. G. Quinn, J. Zhang, and P. E. Hargraves (1998), An effect of dissolved nutrient concentrations on alkenone-based temperature estimates, *Paleoceanography*, *13*(2), 122–126, doi:10.1029/97PA03358.

Farrimond, P., G. Eglinton, and S. C. Brassell (1986), Alkenones in Cretaceous black shales, Blake-Bahama basin, western North Atlantic, *Org. Geochem.*, *10*, 897–903, doi:10.1016/S0146-6380(86)80027-4.

Gartner, S. (1967), Calcareous nannofossils from Neogene of Trinidad, Jamaica, and Gulf of Mexico, *Univ. Kans. Paleontol. Contrib.*, *28*, 1–7.

Gartner, S. (1969), *Hayella* Roth and *Hayella* Gartner, *Micropaleontology*, *15*, 490.

Grassé, P. P. (1952), *Traité de Zoologie, Anatomie, Systématique, Biologie*, vol. 1, 1071 pp., Masson, Paris.

Geisen, M., J. Bollmann, J. O. Herrle, J. Mutterlose, and J. R. Young (1999), Calibration of the random settling technique for calculation of absolute abundance of calcareous nannoplankton, *Micropaleontology*, *45*(4), 437–442.

Gibbs, S., N. Shackleton, and J. R. Young (2004), Identification of dissolution patterns in nannofossil assemblages: A high-resolution comparison of synchronous records from Ceara rise, ODP Leg 154, *Paleoceanography*, *19*, PA1029, doi:10.1029/2003PA000958.

Gong, C., and D. J. Hollander (1997), Differential contribution of bacteria to sedimentary organic matter in oxic and anoxic environments, Santa Monica basin, California, *Org. Geochem.*, *26*, 545–563, doi:10.1016/S0146-6380(97)00018-1.

Gong, C., and D. J. Hollander (1999), Evidence for the differential degradation of alkenones under contrasting bottom water oxygen conditions: Implication for paleotemperature reconstruction, *Geochim. Cosmochim. Acta*, *63*, 405–411, doi:10.1016/S0016-7037(98)00283-X.

Grimalt, J. O., J. Rullkötter, M.-A. Sicre, R. Summons, J. Farrington, H. R. Harvey, M. Goñi, and K. Sawada (2000), Modifications of the $C_{37}$ alkenone and alkenoate composition in the water column and sediment: Possible implications for sea surface temperature estimates in paleoceanography, *Geochem. Geophys. Geosyst.*, *1*(11), 1031, doi:10.1029/2000GC000053.

Hay, W. W., H. Mohler, and M. E. Wade (1966), Calcareous nannofossils from Nal'chik (northwest Caucasus), *Eclogae Geol. Helv.*, *56*, 379–399.

Haq, B. U. (1966), Electron microscope studies on some upper Eocene calcareous nannoplankton from Syria, *Stockholm Contrib. Geol.*, *15*, 23–37.

Haq, B. U. (1976), Coccoliths in cores from the Bellinghausen abyssal plain and Antarctic continental rise (DSDP Leg 35), *Initial Rep. Deep Sea Drill. Proj.*, *35*, 557–567.

Haq, B. U., and W. A. Berggren (1978), Late Neogene calcareous plankton biochronology of the Rio Grande Rise (South Atlantic Ocean), *J. Paleontol.*, *52*, 1167–1194.

Haq, B. U., and G. P. Lohmann (1976), Early Cenozoic calcareous nannoplankton biogeography of the Atlantic Ocean, *Mar. Micropaleontol.*, *1*, 119–197.

Hay, W. W., H. P. Mohler, P. H. Roth, and R. R. Schmidt (1967), Calcareous nannoplankton zonation of the Cenozoic of the Gulf Coast and Caribbean-Antillean area, and transoceanic correlation, *Trans. Gulf Coast Assoc. Geol. Soc.*, *17*, 428–480.

Henderiks, J. (2008), Coccolithophore size rules—Reconstructing ancient cell geometry and cellular calcite quota from fossil coccoliths, *Mar. Micropaleontol.*, *67*, 143–154, doi:10.1016/j.marmicro.2008.01.005.

Henderiks, J., and M. Pagani (2007), Refining ancient carbon dioxide estimates: Significance of coccolithophore cell size for alkenone-based $pCO_2$ records, *Paleoceanography*, *22*, PA3202, doi:10.1029/2006PA001399.

Henderiks, J., and A. Törner (2006), Reproducibility of coccolith morphometry: Evaluation of spraying and smear slide preparation techniques, *Mar. Micropaleontol.*, *58*, 207–218, doi:10.1016/j.marmicro.2005.11.002.

Jasper, J. P., and J. M. Hayes (1990), A carbon isotope record of $CO_2$ levels during the late Quaternary, *Nature*, *347*, 462–464, doi:10.1038/347462a0.

Jasper, J. P., J. M. Hayes, A. C. Mix, and F. G. Prahl (1994), Photosynthetic fractionation of $^{13}C$ and concentrations of dissolved $CO_2$ in the central equatorial Pacific during the last 255,000 years, *Paleoceanography*, *9*, 781–798, doi:10.1029/94PA02116.

Jerkovic, L. (1970), Noelaerhabdus nov. gen. type d'une nouvelle famille de coccolithphorides fossiles, Noelaerhabdaceae du Miocène supérieur de Yougoslavie, *C. R. Acad. Sci*, *270*, 468–470.

Kamptner, E. (1954), Untersuchungen uber den feinbau der coccolithen, *Arch. Protistenkd.*, *100*, 1–90.

Klaas, C., and D. E. Archer (2002), Association of sinking organic matter with various types of mineral ballast in the deep sea: Implications for the rain ratio, *Global Biogeochem. Cycles*, *16*(4), 1116, doi:10.1029/2001GB001765.

Laws, E. A., B. N. Popp, R. R. Bidigare, M. C. Kennicutt, and S. A. Macko (1995), Dependence of phytoplankton carbon isotopic composition on growth rate and $[CO_2]_{aq}$: Theoretical considerations and experimental results, *Geochim. Cosmochim. Acta*, *59*, 1131–1138, doi:10.1016/0016-7037(95)00030-4.

Loeblich, A. R., and H. Tappan (1978), The coccolithophorid genus *Calcidiscus* Kamptner and its synonyms, *J. Paleontol.*, *52*, 1390–1392.

Lohmann, H. (1902), Die Coccolithophoridae, eine monographie der coccolithen bildenden flagellaten, zugleich ein beitrat zur kenntnis des Mittelmeerauftriebs, *Arch. Protistenkd.*, *1*, 89–165.

Marlowe, I. T., S. C. Brassell, G. Eglinton, and J. C. Green (1984), Long chain unsaturated kenones and esters in living algae and marine sediments, *Org. Geochem.*, *6*, 135–141, doi:10.1016/0146-6380(84)90034-2.

Marlowe, I. T., S. C. Brassell, G. Eglinton, and J. C. Green (1990), Long-chain alkenones and alkyl alkenoates and the fossil coccolith record of marine sediments, *Chem. Geol.*, *88*, 349–375, doi:10.1016/0009-2541(90)90098-R.

Martrat, B., J. O. Grimalt, C. Lopez-Martinez, I. Cacho, F. J. Sierro, J. A. Flores, R. Zahn, M. Canals, J. H. Curtis, and D. A. Hodell (2004), Abrupt temperature changes in the western Mediterranean over the past 250,000 years, *Science*, *306*, 1762–1765, doi:10.1126/science.1101706.

Mukhopadhyay, P. K., J. Rullkötter, and D. H. Welte (1983), Facies and diagenesis of organic matter in sediments from the Brazil basin and the Rio Grande Rise, Deep Sea Drilling Project Leg 72, *Initial Rep. Deep Sea Drill. Proj.*, *72*, 821–828, doi:10.2973/dsdp.proc.72.138.1983.

Müller, C. (1970), Nannoplankton-zonen der unteren-meeresmolasse Bayerns, *Geol. Bavarica*, *63*, 107–118.

Müller, P. J., M. Cepek, G. Ruhland, and R. R. Schneider (1997), Alkenone and coccolithophorid species changes in late Quaternary sediments from the Walvis Ridge: Implications for the alkenone paleotemperature method, *Palaeogeogr. Palaeoclimatol. Palaeoecol.*, *135*, 71–96, doi:10.1016/S0031-0182(97)00018-7.

Müller, P. J., G. Kirst, G. Rulhand, I. von Storch, and A. Rosell-Melé (1998), Calibration of the alkenone paleotemperature index $U^{K'}_{37}$ based on core-tops from the eastern South Atlantic and the global ocean (60°N–60°S), *Geochim. Cosmochim. Acta*, *62*(10), 1757–1772, doi:10.1016/S0016-7037(98)00097-0.

Murray, G., and V. H. Blackman (1898), On the nature of the coccospheres and rhabdospheres, *Philos. Trans. R. Soc. B*, *190*, 427–441.

Pagani, M. (2002), The alkenone-$CO_2$ proxy and ancient atmospheric $CO_2$, in *Understanding Climate Change: Proxies, Chronology, and Ocean–atmosphere Interactions: Papers of a Theme*, *Philos. Trans. R. Soc. A*, 360, 609–632.

Pagani, M., M. A. Arthur, and K. H. Freeman (1999), Miocene evolution of atmospheric carbon dioxide, *Paleoceanography*, *14*(3), 273–292, doi:10.1029/1999PA900006.

Pagani, M., K. H. Freeman, and M. A. Arthur (2000a), Isotope analyses of molecular and total organic carbon from Miocene sediments, *Geochim. Cosmochim. Acta*, *64*, 37–49, doi:10.1016/S0016-7037(99)00151-9.

Pagani, M., M. A. Arthur, and K. H. Freeman (2000b), Variations in Miocene phytoplankton growth rates in the southwest Atlantic: Evidence for changes in ocean circulation, *Paleoceanography*, *15*, 486–496, doi:10.1029/1999PA000484.

Pagani, M., J. C. Zachos, K. H. Freeman, B. Tripple, and S. Bohaty (2005), Marked decline in atmospheric carbon dioxide concentrations during the Paleogene, *Science*, *309*, 600–603, doi:10.1126/science.1110063.

Pahnke, K., and J. P. Sachs (2006), Sea surface temperatures of southern midlatitudes 0–160 kyr B.P., *Paleoceanography*, *21*, PA2003, doi:10.1029/2005PA001191.

Popp, B. N., E. A. Laws, R. R. Bidigare, J. E. Dore, K. L. Hanson, and S. G. Wakeham (1998), Effect of phytoplankton cell geometry on carbon isotopic fractionation, *Geochim. Cosmochim. Acta*, *62*, 69–77, doi:10.1016/S0016-7037(97)00333-5.

Prahl, F. G., and S. G. Wakeham (1987), Calibration of unsaturation patterns in long-chain ketone compositions for paleotemperature assessment, *Nature*, *330*, 367–369, doi:10.1038/330367a0.

Prahl, F. G., G. V. Wolfe, and M. A. Sparrow (2003), Physiological impacts on alkenone paleothermometry, *Paleoceanography*, *18*(2), 1025, doi:10.1029/2002PA000803.

Pujos-Lamy, A. (1977), Essai d'établissement d'une biostratigraphie du nannoplancton calcaire dans le Pleistocène de l'Atlantique Nord-oriental, *Boreas*, *6*, 323–331, doi:10.1111/j.1502-3885.1977.tb00297.x.

Riebesell, U., A. T. Revill, D. G. Hodsworth, and J. K. Volkman (2000), The effects of varying $CO_2$ concentration on lipid composition and carbon isotope fractionation in *Emiliania huxleyi*, *Geochim. Cosmochim. Acta*, *64*, 4179–4192, doi:10.1016/S0016-7037(00)00474-9.

Rontani, J. F., and S. G. Wakeham (2008), Alteration of alkenone unsaturation ratio with depth in the Black Sea: Potential roles of stereomutation and aerobic biodegradation, *Org. Geochem.*, *39*(9), 1259–1268, doi:10.1016/j.orggeochem.2008.06.002.

Roth, P. H. (1970), Oligocene calcareous nannoplankton biostratigraphy, *Eclogae Geol. Helv.*, *63*, 799–881.

Roth, P. H., and W. T. Coulbourn (1982), Floral and solution patterns of coccoliths in surface sediments of the North Pacific, *Mar. Micropaleontol.*, *7*, 1–52, doi:10.1016/0377-8398(82)90014-7.

Sáez, A. G., I. Probert, J. R. Young, B. Edvardsen, W. Eikrem, and L. K. Medlin (2004), A review of the phylogeny of the Haptophyta, in *Coccolithophores: From Molecular Processes to Global Impact*, edited by H. R. Thierstein and J. R. Young, pp. 251–269, Springer, Berlin.

Schiller, J. (1930), *Coccolithineae, Dr. L. Rabenhorst's Kryptogamen-Flora von Deutschland, Osterreich und der Schweiz Ser.*, vol. 10, edited by L. Rabenhorst, pp. 89–273, Akad. Verl., Leipzig, Germany.

Seki, O., G. L. Foster, D. N. Schmidt, A. Mackensen, K. Kawamura, and R. D. Pancost (2010), Alkenone and boron-based Pliocene $pCO_2$ records, *Earth Planet. Sci. Lett.*, *292*, 201–211, doi:10.1016/j.epsl.2010.01.037.

Sun, M. Y., and S. G. Wakeham (1994), Molecular evidence for degradation and preservation of organic matter in the anoxic Black Sea basin, *Geochim. Cosmochim. Acta*, *58*, 3395–3406, doi:10.1016/0016-7037(94)90094-9.

Tan, S. H. (1927), Over de samenstelling en het onstaan van krijt en mergelgesteenten van de Molukken, *Jaarbk. Mijnwezen Ned. Indie*, *55*, 111–122.

Theodoridis, S. (1984), *Calcareous Nannofossil Biozonation of the Miocene and Revision of the Helicoliths and Discoasters*, *Utrecht Micropaleontol. Bull. Ser.*, vol. 32, 1–271, State Univ. of Utrecht, Utrecht, Germany.

Thierstein, H. R., K. R. Geitzenauer, B. Molfino, and N. J. Shackleton (1977), Global synchroneity of late Quaternary coccolith datum levels: Validation by oxygen isotopes, *Geology*, *5*, 400–404, doi:10.1130/0091-7613(1977)5<400:GSOLQC>2.0.CO;2.

Volkman, J. K., G. Eglinton, E. D. S. Corner, and T. E. V. Forsberg (1980), Long-chain alkenes and alkenones in the marine coccolithphorid *Emiliania huxleyi*, *Phytochemistry*, *19*, 2619–2622, doi:10.1016/S0031-9422(00)83930-8.

Volkman, J. K., S. M. Barrett, S. I. Blackburn, and E. L. Sikes (1995), Alkenones in *Gephyrocapsa oceanica*: Implications for studies of paleoclimate, *Geochim. Cosmochim. Acta*, *59*, 513–520, doi:10.1016/0016-7037(95)00325-T.

Wallich, G. C. (1877), Observations on the coccosphere, *Ann. Mag. Nat. Hist.*, *19*, 342–350.

Weaver, P. P. E., M. R. Chapman, G. Eglinton, M. Zhao, D. Rutledge, and G. Read (1999), Combined coccolith, foraminiferal, and biomarker reconstruction of paleoceanographic conditions over the past 120 kyr in the northern North Atlantic (59°N, 23°W), *Paleoceanography*, *14*, 336–349, doi:10.1029/1999PA900009.

Wise, S. W. (1973), Calcareous nannofossils from cores recovered during Leg 18, Deep Sea Drilling Project: Biostratigraphy and observations on diagenesis, *Initial Rep. Deep Sea Drill. Proj.*, *18*, 569–615.

Young, J. R. (1990), Size variation of Neogene *Reticulofenestra* coccoliths from Indian Ocean DSDP cores, *J. Micropaleontol.*, *9*, 71–85, doi:10.1144/jm.9.1.71.

Young, J. R. (1998), Neogene, in *Calcareous Nannofossil Biostratigraphy*, edited by P. R. Bown, pp. 225–265, Chapman and Hall, Cambridge, U. K., doi:10.1007/978-94-011-4902-0_8.

Young, J. R., and P. R. Bown (1997), Cenozoic calcareous nannoplankton classification, *J. Nannoplankton Res.*, *19*, 36–47.

Young, J. R., M. Geisen, L. Cros, A. Kleijne, I. Probert, C. Sprengel, and J. B. Ostergaard (2003), A guide to extant coccolithophore taxonomy, *J. Nannoplankton Res. Spec. Issue 1*, 1–132.

Young, J. R., M. Geisen, and I. Probert (2005), A review of selected aspects of coccolithophore biology with implications for palaeobiodiversity estimation, *Micropaleontology*, *51*(4), 267–288, doi:10.2113/gsmicropal.51.4.267.

V. Grossi, E. Mattioli, and J. Plancq, Laboratoire de Géologie de Lyon, UMR 5276, CNRS, Université Lyon 1, Ecole Normale Supérieure Lyon, Batiment Géode, 2 rue Raphaël Dubois, Campus scientifique de la DOUA, Villeurbanne F-69622, France. (julien.plancq@pepsmail.univ-lyon1.fr)

J. Henderiks, Paleobiology Program, Department of Earth Sciences, Uppsala University, Villavägen 16, SE-752 36 Uppsala, Sweden.

L. Simon, Laboratoire d'Ecologie des Hydrosystèmes Naturels et Anthropisés, UMR 5023, CNRS, Université Claude Bernard Lyon 1, 6 rue Dubois, Campus scientifique de la DOUA, Villeurbanne F-69622, France.